

# DocuServe

## Electronic Delivery Cover Sheet

### **WARNING CONCERNING COPYRIGHT RESTRICTIONS**

The copyright law of the United States (Title 17, United States Code) governs the making of photocopies or other reproductions of copyrighted materials. Under certain conditions specified in the law, libraries and archives are authorized to furnish a photocopy or other reproduction. One of these specified conditions is that the photocopy or reproduction is not to be "used for any purpose other than private study, scholarship, or research". If a user makes a request for, or later uses, a photocopy or reproduction for purposes in excess of "fair use", that user may be liable for copyright infringement. This institution reserves the right to refuse to accept a copying order if, in its judgment, fulfillment of the order would involve violation of copyright law.

Caltech Library Services

Association  $\text{CH}\cdots\pi$  and No van der Waals Contacts at the Lowest Limits of Crystalline Benzene I and II Stability Regions<sup>†</sup>Andrzej Katrusiak,\* Marcin Podsiadło, and Armand Budzianowski<sup>‡</sup>Faculty of Chemistry, Adam Mickiewicz University, Grunwaldzka 6, 60-780 Poznań, Poland. <sup>‡</sup>Present address: ICM, The University of Warsaw, Żwirki i Wigury 93, 02-089 Warsaw, Poland.

Received February 25, 2010; Revised Manuscript Received May 21, 2010

**ABSTRACT:** Molecular arrangements have been determined at the lowest limits of pressure ranges of benzene phase I, at 0.15 GPa, and phase II at 0.91 and 0.97 GPa, all at 295 K. All intermolecular contacts both in phase I and phase II to about 1.0 GPa exceed the sums of van der Waals radii; however, the transition between phases I and II does not affect the pattern of  $\text{CH}\cdots\pi$ (arene) hydrogen bonds. In phase I the molecules are  $\text{CH}\cdots\pi$  bonded approximately perpendicular into sheets, and there are substantial voids between the molecules within the sheets. The mechanism of transition to phase II involves a collapse of the voids, simultaneous with a shift of the  $\text{CH}\cdots\pi$  bonded sheets. The thickness of sheets increases, which partly compensates the volume reduction due to the voids collapse; hence, the transition exhibits a large hysteresis of two GPa and a sluggish character at 295 K. No other phases of benzene have been observed between 0.15 and 5.0 GPa.

## Introduction

Benzene belongs to the most common and best known organic compounds, since its simple and highly symmetric molecular structure inspired the concept of aromaticity; the molecular structure of benzene was thoroughly studied theoretically and experimentally; however, the intermolecular interactions and molecular association of benzene molecules still remain controversial. It was established that at 270 K benzene freezes in orthorhombic phase I, space group  $Pbca$ <sup>1–3</sup> was confirmed at 218 K and is stable to 138 K.<sup>4</sup> This symmetry has been confirmed for perdeuterobenzene at 123, 15,<sup>5</sup> and 4 K.<sup>6</sup> Bridgman discovered phase II of benzene by calorimetric measurements, which he conducted in the 373–473 K range up to 1.18 GPa, and determined the transition-boundary slope between phases I and II,  $dT_c/dp$ .<sup>7</sup> The phases I/II boundary outside those limits, below 373 °C and above 1.18 GPa, could be estimated from Bridgman's  $dT_c/dp$  slope (Figure 17 in Ref. 7) to occur at 293 K above 1.3 GPa. Bridgman could not follow the transition boundary by the calorimetric method below 373 K and above 1.18 GPa. His compressibility measurements of benzene at 323 K up to 5 GPa suggested a very small volume change, of –0.9% at the phase I/II transition, practically undetectable in the recorded results.<sup>8</sup> Thiéry & Léger (1988)<sup>9</sup> observed that the transition between phases I and II required triggering by a temperature of about 373 K, while at room temperature the transition proceeded in a sluggish way and required a much higher pressure of about 3 GPa to occur. They referred to similar observations by Bridgman,<sup>8</sup> to their own spectroscopic studies and X-ray powder diffraction measurements compared to the previously determined crystal structures of benzene I<sup>10</sup> and benzene II.<sup>11</sup> In the following studies, about seven crystalline phases of benzene were proposed up to the limit of about 700 K and 25 GPa, when benzene polymerizes;<sup>12</sup> however, most recently the phase diagram was simplified to three phases only.<sup>13,14</sup> The structure of benzene II was one of the first ones determined using a

single-crystal and a diamond anvil cell: it is monoclinic, space group  $P2_1/c$ .<sup>11</sup> The determination of the benzene II structure, obtained by reorienting the rigid molecule about the inversion center and confronting the model against 19 reflections recorded photographically and against intermolecular interactions, was a milestone in the high-pressure analysis at that time.<sup>11</sup> Pressure of the crystal was assessed visually as 2.5 GPa, while the authors admitted its huge uncertainty of 2.0 GPa.<sup>15</sup> In that pioneering work, clear structural relations between phases I and II were noted. The present study was aimed at clarifying the nature of the transition between phases I and II, at determining the crystal structures of benzene phases I and II at their lowest possible pressure at 295 K, in order to describe the molecular interactions and their changes just above freezing and at the transition between phases I and II, and at confirming the absence of other benzene phases in the pressure range to 5 GPa.

## Experimental Section

Benzene (m.p. 279 K), analytical grade from Polskie Odczynniki Chemiczne, was used without further purification. This liquid was loaded into a modified Merrill-Bassett<sup>16</sup> diamond-anvil cell (DAC) and in situ crystallized. The gasket-hole in the 0.3 mm thick steel foil was spark-eroded and preindented to ca. 0.27 mm; the initial diameter of the chamber was 0.45 mm. The sample froze at 0.05(5) GPa/295 K, which is consistent with the freezing pressure of benzene determined by Bridgman<sup>7,17</sup> (Figure 1a). Pressure calibration by the ruby-fluorescence method<sup>18,19</sup> using a BETSA PRL spectrometer afforded an accuracy of 50 MPa. The crystallization triggered the characteristic process of spontaneous growth of benzene single-crystal grains inside the DAC (Figure 1a–c), previously observed at 296 K and 0.07 GPa.<sup>20</sup> Then the DAC chamber was heated to ca. 300 K (Figure 1d,e), and the pressure was increased to ca. 1 GPa (Figure 1f). When the chamber was heated to ca. 550 K, the crystal turned opaque, which marked a solid–solid phase transition to benzene II (Figure 1g). This polycrystalline mass was further heated to ca. 630 K, and two single crystals were grown by cooling the DAC slowly to room temperature (Figure 1h–l). At 295 K pressure settled to 0.91(5) GPa, and the crystal shown in Figure 1l was studied by X-ray diffraction. After the diffraction experiment, the DAC was warmed up and annealed for 17 h at 400 K for reducing the strains in the benzene II crystal. This crystal was used for the next X-ray diffraction experiment at 0.97(5) GPa/295 K. After collecting

<sup>†</sup> This paper is dedicated in memory of D. W. J. Cruickshank (1924–2007)<sup>\*</sup> To whom correspondence should be addressed. E-mail: katran@amu.edu.pl.

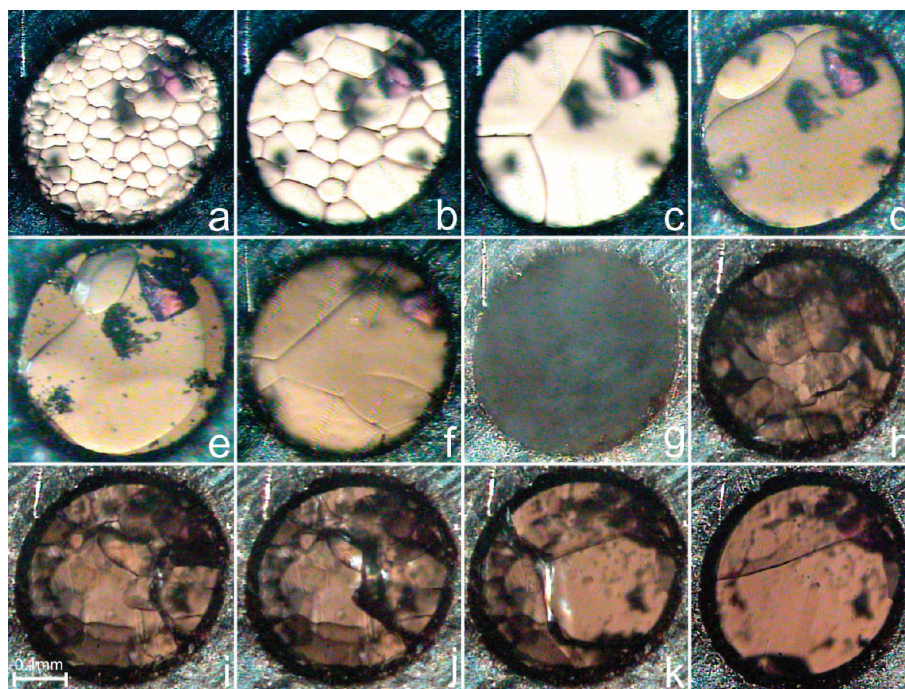


**Figure 1.** The process of obtaining benzene II sample in the DAC chamber: (a–c) spontaneous growth of benzene I grains at 295 K and ca. 0.1 GPa; (d, e) the benzene I sample heated to ca. 300 K, and (f) squeezed to ca. 1 GPa at 300 K; (g) solid–solid transition between phases I and II at ca. 550 K; (h) the sample heated to ca. 630 K and (i–k) cooled slowly; (l) two single crystals in phase II at 0.91 GPa/295 K, used for the X-ray diffraction study. Ruby-chips for pressure calibration are at the upper right edge of the high-pressure chamber.

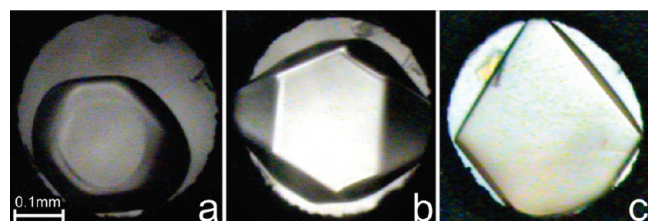


**Figure 2.** The crystal habits of benzene I at 300 K/0.1 GPa (a); 330 K/0.2 GPa (b); and benzene II at 400 K/1.3 GPa (c).

the X-ray data, the pressure was reduced to 0.15(5) GPa and the subsequent diffraction measurement confirmed the crystal structure of benzene I. A series of benzene crystals was grown in the pressure range between 1 and 5 GPa and temperature up to 630 K, and their structures were checked by X-ray diffraction, but no other phases than I and II were found. The habits of the benzene I and benzene II crystals are shown in Figure 2. The rounded morphology of the heated benzene I crystals<sup>20</sup> (Figure 1a–e) mimics the reverse roughening transition<sup>21</sup> in this phase.

The single-crystal X-ray data at 0.15, 0.91, and 0.97 GPa were collected using a KM-4 CCD diffractometer with graphite-monochromated MoK $\alpha$  radiation. The centering of the DAC was performed by the gasket-shadowing method.<sup>22</sup> The reflections were collected with the  $\omega$ -scan technique, 0.70° frame widths and 35 s exposures.<sup>22</sup> Program suite *CrysAlis*<sup>23</sup> was used for data collections, determination of the *UB*-matrices, initial data reductions, and *Lp* corrections. In all the measurements, the reflection intensities have been corrected for the effects of absorption of X-rays by the DAC, shadowing of the beams by the gasket edges and absorption of the sample crystals themselves.<sup>24,25</sup> The C<sub>6</sub>H<sub>6</sub> structures were solved by direct methods using program *SHELXS-97* and refined with anisotropic displacement parameters for C-atoms by program *SHELXL-97*.<sup>26</sup> The H-atoms were positioned with the C–H bond length restrained to 0.93 Å and their isotropic displacement parameters set at 1.2 times *U*<sub>eq</sub> of C atoms. Selected details of the structures refinements and crystal data are listed in Table 1. The compressibility measurement of benzene was performed up to ca. 2 GPa in a

piston-and-cylinder apparatus,<sup>27</sup> with an initial volume of ca. 8.4 mL. Program *CrystalExplorer*<sup>28</sup> and a PC were used for calculations of the electrostatic potential on the molecular surfaces of benzene. Electrostatic potential<sup>29</sup> was mapped onto the molecular surfaces defined as a 0.001 a.u. electron-density envelope.<sup>30</sup>

## Discussion

The molecular volume of benzene I measured by X-ray diffraction at 0.15 (this work), 0.7, and 1.1 GPa<sup>20</sup> well agrees with that measured in the piston-cylinder press (see Figure 3). The liquid–solid phase transition is marked by the volume discontinuity at 0.07 GPa, consistent with the freezing pressure determined by Bridgman.<sup>7,17</sup> No other volume anomalies, which could be interpreted as a solid–solid phase transition, have been detected up to 2 GPa in the compression data. Our results are consistent with the previously described sluggish nature of the I/II phase transition at room temperature, and a much higher pressure of ca. 3 GPa required for triggering it in a large-volume compressibility measurements.<sup>8,9</sup> Thus, it is likely that in a pressure range up to 2.0 GPa the crystal remained in phase I (overpressed above ca. 1.3 GPa). On the other hand, the molecular volume of benzene derived from Piermarini's et al. (1969),<sup>11</sup> single-crystal structure would fit to the volume at about 1.55 GPa in the plot in Figure 3. A possible reason of this discrepancy may be an uncertainty in the visual pressure estimation, of 2.5(20) GPa,<sup>15</sup> before a highly efficient ruby-fluorescence calibration method was described by Piermarini et al. several years later.<sup>19</sup>

The main difference in the molecular arrangement in benzene I and II is in the mutual orientation of molecules forming CH $\cdots\pi$ (arene) contacts. In benzene I (0.15 GPa/295 K), the angle between the molecular planes is equal to 82.74°, while in benzene II at 0.91 GPa/295 K it is 62.09° (Figure 4), and in this respect the phase transition can be considered as a collapse of the benzene I structure. In phase I the CH $\cdots\pi$ (arene) bonds



**Table 1.** Crystal Data and Details of the Refinements of C<sub>6</sub>H<sub>6</sub> at 0.15 GPa/295 K (Phase I), 0.91 GPa/295 K and 0.97 GPa/295 K (Phase II)

	C <sub>6</sub> H <sub>6</sub> phase I	C <sub>6</sub> H <sub>6</sub> phase II	C <sub>6</sub> H <sub>6</sub> phase II
temperature (K)	295(2)	295(2)	295(2)
pressure (GPa)	0.15(5)	0.91(5)	0.97(5)
formula weight	78.11	78.11	78.11
crystal color	colorless	colorless	colorless
crystal size (mm)	0.40 × 0.40 × 0.25	0.40 × 0.40 × 0.25	0.40 × 0.40 × 0.25
crystal system	orthorhombic	monoclinic	monoclinic
space group	<i>Pbca</i>	<i>P2<sub>1</sub>/c</i>	<i>P2<sub>1</sub>/c</i>
unit cell dimensions (Å; °)	<i>a</i> = 7.3801(15) <i>b</i> = 9.5154(19) <i>c</i> = 6.9029(14)	<i>a</i> = 5.5146(11) <i>b</i> = 5.4951(11) <i>c</i> = 7.6536(15) $\beta$ = 110.59(3)	<i>a</i> = 5.5220(11) <i>b</i> = 5.4396(11) <i>c</i> = 7.6726(15) $\beta$ = 110.55(3)
volume (Å <sup>3</sup> )	484.75(17)	217.11(7)	215.81(7)
<i>Z</i>	4	2	2
<i>D<sub>x</sub></i> (g cm <sup>−3</sup> )	1.070	1.195	1.202
wavelength, MoK $\alpha$ (Å)	$\lambda$ = 0.71073	$\lambda$ = 0.71073	$\lambda$ = 0.71073
absorption coefficient (mm <sup>−1</sup> )	0.06	0.07	0.07
<i>F</i> (000) (e)	168	84	84
2 $\theta$ max (°)	57.24	56.76	56.70
min/max indices <i>h,k,l</i>	−7/8, −12/12, −6/6	−7/7, −2/2, −9/9	−7/7, −2/2, −9/9
reflections collected/unique	2141/257	915/138	938/138
<i>R</i> <sub>int</sub>	0.0816	0.0604	0.0722
observed reflections ( <i>I</i> > 4 $\sigma$ ( <i>I</i> ))	161	124	122
data/parameters	257/29	138/29	138/29
goodness of fit on <i>F</i> <sup>2</sup>	1.214	1.249	1.213
final <i>R</i> <sub>1</sub> indices ( <i>I</i> > 4 $\sigma$ ( <i>I</i> ))	0.0852	0.0804	0.0761
<i>R</i> <sub>1</sub> / <i>wR</i> <sub>2</sub> indices (all data)	0.1352/0.2547	0.0845/0.2266	0.0819/0.2089
$\Delta\sigma_{\max}$ , $\Delta\sigma_{\min}$ (e Å <sup>−3</sup> )	0.08, −0.08	0.12, −0.09	0.14, −0.11
weighting parameters <i>w</i> ; <i>y</i> <sup><i>a</i></sup>	0.0996; 0.10	0.1071; 0.17	0.0908; 0.19
absorption corrections	DAC, gasket and sample crystal	DAC, gasket and sample crystal	DAC, gasket and sample crystal
DAC transmission min/max	0.90/1.00	0.91/1.00	0.91/1.00
gasket shadowing min/max	0.59/0.95	0.62/0.96	0.62/0.96
sample transmission min/max	0.98/0.99	0.98/0.99	0.98/0.99
extinction method	<i>SHELXL</i>	<i>SHELXL</i>	<i>SHELXL</i>
extinction coefficient	0.07(5)	0.6(3)	1.0(3)

$$^a w = 1/(\sigma^2(F_o^2) + x^2P^2 + yP), \text{ where } P = (\max(F_o^2, 0) + 2Fc^2)/3.$$

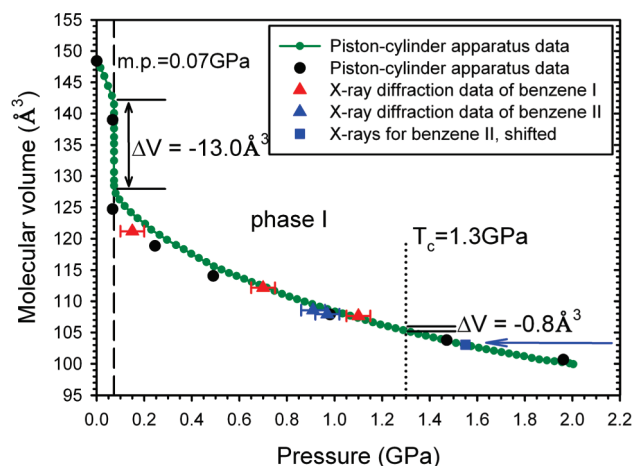


**Figure 3.** Molecular volume of C<sub>6</sub>H<sub>6</sub> at 295 K in the function of pressure. The freezing pressure is marked by the volume jump at 0.07 GPa. Green circles represent the molecular volume measured in the piston-cylinder press, while red and blue triangles mark those from high-pressure X-ray single-crystal diffraction study of benzene I and II, respectively. Black circles represent the lower pressure range of data from the piston-cylinder press after Bridgman, 1949.<sup>17</sup> The molecular volume determined by Piermarini et al., 1969<sup>11</sup> (blue square) has been shifted, as indicated by the blue arrow, from 2.5 GPa (outside the scale) to 1.55 GPa, to match the compressibility measurements.

arrange the molecules nearly perpendicular, and they enclose voids in the sheets running along crystal plane (010), shown in Figures 4 and 5.

The collapse of the voids in phase II (Figure 5) coincides with shear shifts of the CH $\cdots\pi$  bonded sheets, parallel to the

crystal plane (010) in phase I and plane (100) in phase II. At this transition, the “thickness” of the sheets increases from 4.76 Å at 0.15 GPa to 5.18 Å in benzene II at 0.91 GPa, as the molecules penetrate deeper into the voids of neighboring sheets in phase I than in phase II, and also the tilts of the molecules with respect to the sheets change. Consequently, the volume reduction due to the collapse of voids is partly compensated. According to Bridgman,<sup>8</sup> the relative  $\Delta V$  at the I/II transition is  $-0.9\%$ . It agrees with the volume change of  $-0.8\%$  determined from our X-ray diffraction measurements of lattice dimensions in the under-pressurized phase II at 0.91 and 0.97 GPa, compared with our piston-cylinder results and the crystal volume of phase I determined by X-ray diffraction (Figure 3).<sup>20</sup> In our compressibility measurement, no  $\Delta V$  was observed about 1.3 GPa, most likely due to the overpressurized phase I fully or partly persisting to over 2.0 GPa at 295 K.

The volume per molecule for benzene I at 0.15 GPa/295 K is equal 121.19 Å<sup>3</sup>, while for benzene II at 0.91 GPa/295 K it is 108.56 Å<sup>3</sup>. This volume difference is reflected in the shortest intermolecular distances in both structures. A striking feature of the benzene structure in phase I is that there are no intermolecular contacts shorter than the sums of van der Waals radii (Figure 6; Table 2). The shortest CH $\cdots$ C contacts at 0.15 GPa/295 K are about 0.14 Å longer than the sum of van der Waals radii of H and C (1.2 and 1.7 Å, respectively, according to Bondi, 1964<sup>31</sup>). Surprisingly, CH $\cdots$ C contacts in the low temperature structure at 0.1 MPa/218 K are somewhat shorter than at 0.15 GPa/295 K (Figure 6). Even at 1.5 GPa/295 K, all intermolecular C $\cdots$ C distances remain longer than the sum of van der Waals radii. Thus, the structures of

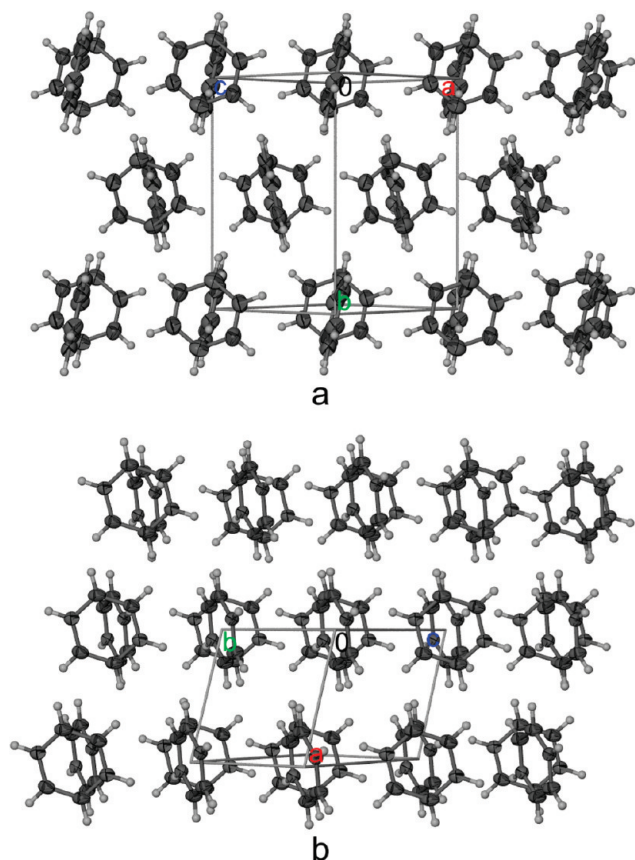


**Figure 4.** The crystal structure of benzene I (a) and benzene II (b) viewed along the  $\text{CH}\cdots\pi(\text{arene})$  hydrogen-bonded sheets.

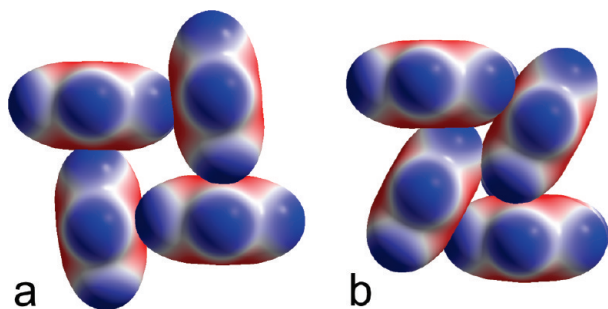


**Figure 5.** The molecular arrangement for benzene I at 0.15 GPa/295 K (a), and benzene II at 0.91 GPa/295 K (b). The electrostatic potential, shown on the molecular surfaces defined as 0.001 a.u. of electron density, ranges from  $-0.015$  a.u. (red) to  $0.015$  a.u. (blue).

**Table 2.** Dimensions of the Shortest Intermolecular  $\text{C}-\text{H}\cdots\pi(\text{arene})$  and  $\text{C}-\text{H}\cdots\text{C}$  Contacts Observed in (a) Benzene I at 0.15 GPa/295 K and (b) Benzene II at 0.91 GPa/295 K (see also Figure S2)<sup>a</sup>

D-H...A	H...A (Å)	D...A (Å)	D-H...A (deg)	symmetry code
phase I at 0.15 GPa/295 K				
C3-H3... $\pi(\text{arene})$	2.957	3.772	147.24	$0.5 + x, y, 0.5 - z$
C2-H2...C1	3.042	3.751	134.28	$0.5 + x, y, 0.5 - z$
C2-H2...C1	3.074	3.750	131.04	$x, 0.5 - y, 0.5 + z$
phase II at 0.91 GPa/295 K				
C2-H2... $\pi(\text{arene})$	2.802	3.506	133.29	$x, 0.5 - y, 0.5 + z$
C1-H1...C3	3.063	3.602	118.65	$-1 - x, -y, -z$
C1-H1...C3	3.069	3.874	145.78	$-1 - x, -0.5 + y, -0.5 - z$

<sup>a</sup> The ring centroid is denoted as the  $\pi(\text{arene})$  symbol in the table below. The symmetry codes of the acceptor atoms are given.

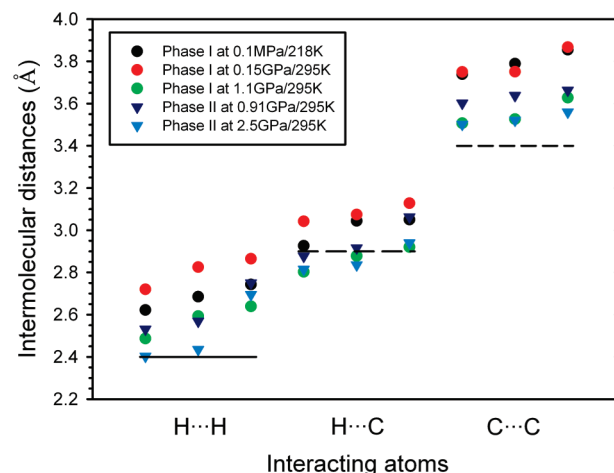


**Figure 6.** The evolution of the shortest  $\text{H}\cdots\text{H}$ ,  $\text{H}\cdots\text{C}$ , and  $\text{C}\cdots\text{C}$  intermolecular distances with temperature and pressure in benzene I and II. The horizontal lines mark the sums of van der Waals radii for relevant atoms.<sup>31</sup>

benzene I and II provide a direct observation that in the crystal without strong intermolecular forces all intermolecular contacts stabilize at distances considerably longer than sums of van der Waals radii. It was shown that distances of optimum stability are considerably longer than the van der Waals contacts observed in molecular crystals,<sup>32,33</sup> whereas the shortest of contacts in molecular crystals indeed have been used for deriving generally accepted van der Waals radii.<sup>34,35</sup>

## Conclusions

In conclusion, the first determination of the structure of benzene II<sup>11</sup> is very consistent with both presently obtained structural results at 0.91 and 0.97 GPa. The mechanism of the benzene I/II phase transition can be described as a collapse of the voids between  $\text{C}-\text{H}\cdots\pi(\text{arene})$  bonded molecules in phase I, and shifts of the neighboring sheets. Because of the elimination of the voids, the interpenetration of molecules into the neighboring voids decreases, which increases the thickness of the sheets, and partly compensates the volume change of the voids collapse, hence the small transition volume change between benzene I and II, the sluggish nature of the phase transition, and its large pressure hysteresis. These determinations of the benzene I and II structures at approximately identical conditions (of about 1.0 GPa) as well as the determination of benzene I at 0.15 GPa reveal yet another important feature of this molecular compound. There are no van der Waals contacts in the lowest-pressure (0.15 GPa) and highest-temperature (218 K) structures of benzene I, and other benzene structures are similarly loose in this sense. These observations are in line with the recent results on the relations between the van der Waals radii and energetical minima of intermolecular interactions in crystals.<sup>32,33,36,37</sup> Most importantly, it illustrates the role of weak interactions for the molecular aggregation, even beyond the closest contacts in crystals. Finally, in the range of temperature and pressure investigated, between 295 and 670 K and 0.1 MPa to 5.0 GPa, no other phases than benzene I and II were obtained, consistently with recent studies on transformations of benzene in high temperature, above 500 K, and high pressure.<sup>13,14</sup>

**Acknowledgment.** This study was supported by the Polish Ministry of Scientific Research, Grant No. N204 1956 33.

Dr. Marcin Podsiadło acknowledges the reception of the scholarship from the Foundation for Polish Science in 2010.

**Supporting Information Available:** Isostructural relation between benzene phases I and II (Figure S1); the shortest intermolecular C–H··· $\pi$ (arene) and C–H···C distances observed in benzene I at 0.15 GPa/295 K and benzene II at 0.91 GPa/295 K (Figure S2). Crystallographic data in CIF format available free of charge via the Internet at <http://pubs.acs.org>.

## References

- (1) Cox, E. G. *Proc. R. Soc. A* **1932**, *135*, 491–497.
- (2) Cox, E. G.; Smith, J. A. S. *Nature* **1954**, *173*, 75.
- (3) Cox, E. G.; Cruickshank, D. W. J.; Smith, J. A. S. *Proc. R. Soc. London A* **1958**, *247*, 1–21.
- (4) Bacon, G. E.; Curry, N. A.; Wilson, S. A. *Proc. R. Soc. A* **1964**, *279*, 98–110.
- (5) Jeffrey, G. A.; Ruble, J. R.; McMullan, R. K.; Pople, J. A. *Proc. R. Soc. London, Ser. A* **1987**, *414*, 47–57.
- (6) David, W. I. F.; Ibberson, R. M.; Jeffrey, G. A.; Ruble, J. R. *Physica B: Condensed Matter* **1992**, *180*, 597–600.
- (7) Bridgman, P. W. *Phys. Rev.* **1914**, *3*, 126–141, 153–203.
- (8) Bridgman, P. W. *J. Chem. Phys.* **1941**, *9*, 794–797.
- (9) Thiéry, M. M.; Léger, J. M. *J. Chem. Phys.* **1988**, *89*, 4255–4271.
- (10) Weir, C. E.; Piermarini, G. J.; Block, S. *J. Chem. Phys.* **1969**, *50*, 2089–2093.
- (11) Piermarini, G. J.; Mighell, A. D.; Weir, C. E.; Block, S. *Science* **1969**, *165*, 1250–1255.
- (12) Pruzan, Ph.; Chervin, J. C.; Thiéry, M. M.; Itié, J. P.; Besson, J. M.; Forgerit, J. P.; Revault, M. *J. Chem. Phys.* **1990**, *92*, 6910–6915.
- (13) Ciabini, L.; Gorelli, F. A.; Santoro, M.; Bini, R.; Schettino, V.; Mezouar, M. *Phys. Rev. B* **2005**, *72*, 094108.
- (14) Ciabini, L.; Santoro, M.; Gorelli, F. A.; Bini, R.; Schettino, V.; Rauei, S. *Nat. Mater.* **2007**, *6* (1), 39–43.
- (15) Block, S.; Weir, C. E.; Piermarini, G. J. *Science* **1970**, *169*, 586–587.
- (16) Merrill, L.; Bassett, W. A. *Rev. Sci. Instrum.* **1974**, *45*, 290–294.
- (17) Bridgman, P. W. *Proc. Am. Acad. Arts Sci.* **1949**, *77*, 129–146.
- (18) Barnett, J. D.; Block, S.; Piermarini, G. J. *Rev. Sci. Instrum.* **1973**, *44*, 1–9.
- (19) Piermarini, G. J.; Block, S.; Barnett, J. D.; Forman, R. A. *J. Appl. Phys.* **1975**, *46*, 2774–2780.
- (20) Budzianowski, A.; Katrusiak, A. *Acta Crystallogr.* **2006**, *B62*, 94–101.
- (21) Giordano, V. M.; Datchi, F. *Phys. Rev. Lett.* **2007**, *99*, 165701.
- (22) Budzianowski, A.; Katrusiak, A. *High-Pressure Crystallography*; Katrusiak, A.; McMillan, P. F., Ed.; Dordrecht: Kluwer Academic Publishers, 2004; pp 101–112.
- (23) *Oxford Diffraction Xcalibur CCD System, CrysAlis Software System*, Version 1.171; Oxford Diffraction Ltd: Abingdon, Oxfordshire, UK, 2004.
- (24) Katrusiak, A. *REDSHABS*; Adam Mickiewicz University: Poznań, Poland, 2003.
- (25) Katrusiak, A. *Z. Kristallogr.* **2004**, *219*, 461–467.
- (26) Sheldrick, G. M. *SHELXS97 and SHELXL97*; University of Göttingen: Germany, 1997.
- (27) Baranowski, B.; Moroz, A. *Pol. J. Chem.* **1982**, *56*, 379–391.
- (28) Grimwood, D. J.; Jayatilaka, D.; McKinnon, J. J.; Spackman, M. A.; Wolff, S. K. *CrystalExplorer*, ver. 2.1; University of Western Australia, Perth, 2008.
- (29) Murray, J. N.; Sen, K. D. *Molecular Electrostatic Potential: Concepts and Applications*; Elsevier: New York, 1996.
- (30) Bader, R. F. W.; Carroll, M. T.; Cheeseman, J. R.; Chang, C. *J. Am. Chem. Soc.* **1987**, *109*, 7968–7979.
- (31) Bondi, A. *J. Phys. Chem.* **1964**, *68*, 441–451.
- (32) Dance, I. *CrystEngComm* **2003**, *5*, 208–221.
- (33) Dance, I. *New J. Chem.* **2003**, *27*, 22–27.
- (34) Kitaigorodskii, A. I. *Molecular Crystals and Molecules*; New York: Academic Press, 1973.
- (35) Nyburg, S. C.; Faerman, C. H. *Acta Crystallogr.* **1985**, *B41*, 274–279.
- (36) Bujak, M.; Podsiadło, M.; Katrusiak, A. *J. Phys. Chem.* **2008**, *B112*, 1184–1188.
- (37) Schiemenz, G. P. *Z. Naturforsch., B: J. Chem. Sci.* **2007**, *62*, 235–243.